ORIGINAL RESEARCH

Involvement of Ca^{2+} in Signaling Mechanisms Mediating Muscarinic Inhibition of M Currents in Sympathetic Neurons

Jin-Young Yoon[1,2] · Won-Kyung Ho[2,3,4]

Abstract

Acetylcholine can excite neurons by suppressing M-type (KCNQ) potassium channels. This effect is mediated by M_1 muscarinic receptors coupled to the G_q protein. Although PIP_2 depletion and PKC activation have been strongly suggested to contribute to muscarinic inhibition of M currents (I_M), direct evidence is lacking. We investigated the mechanism involved in muscarinic inhibition of I_M with Ca^{2+} measurement and electrophysiological studies in both neuronal (rat sympathetic neurons) and heterologous (HEK cells expressing KCNQ2/KCNQ3) preparations. We found that muscarinic inhibition of I_M was not blocked either by PIP_2 or by calphostin C, a PKC inhibitor. We then examined whether muscarinic inhibition of I_M uses multiple signaling pathways by blocking both PIP_2 depletion and PKC activation. This maneuver, however, did not block muscarinic inhibition of I_M. Additionally, muscarinic inhibition of I_M was not prevented either by sequestering of G-protein $\beta\gamma$ subunits from G_α-transducin or anti-$G_{\beta\gamma}$ antibody or by preventing intracellular trafficking of channel proteins with blebbistatin, a class-II myosin inhibitor. Finally, we re-examined the role of Ca^{2+} signals in muscarinic inhibition of I_M. Ca^{2+} measurements showed that muscarinic stimulation increased intracellular Ca^{2+} and was comparable to the Ca^{2+} mobilizing effect of bradykinin. Accordingly, 20-mM of BAPTA significantly suppressed muscarinic inhibition of I_M. In contrast, muscarinic inhibition of I_M was completely insensitive to 20-mM EGTA. Taken together, these data suggest a role of Ca^{2+} signaling in muscarinic modulation of I_M. The differential effects of EGTA and BAPTA imply that Ca^{2+} microdomains or spatially local Ca^{2+} signals contribute to inhibition of I_M.

Keywords KCNQ potassium channel · Muscarinic receptor · Ca^{2+} · PIP_2 · PKC · Sympathetic neurons

Abbreviations

CaM	Calmodulin
G_αTD	G_α-transducin
GFP	Green fluorescent protein
I_M	M channel current
M_1R	M1 muscarinic (acetylcholine) receptor
M channels	M-type (KCNQ/Kv7) K$^+$ channels
NCS-1	Neuronal calcium sensor-1
Oxo-M	Oxotremorine-M
PI	Phosphoinositide
PIP_2	Phosphatidylinositol 4,5-bisphosphate
PI-5-kinase	Phosphoinositide-5-kinase
PKC	Protein kinase C
PLC	Phospholipase C
SCG	Superior cervical ganglion
TTX	Tetrodotoxin

✉ Jin-Young Yoon
jinyoung-yoon@uiowa.edu

1 Department of Internal Medicine, Division of Cardiovascular Medicine, University of Iowa, 285 Newton Rd, 2283 CBRB, Iowa City, Iowa 52242, USA

2 Department of Physiology, Seoul National University College of Medicine, Seoul, Korea

3 Neuroscience Research Institute, Seoul National University College of Medicine, Seoul, Korea

4 Department of Brain and Cognitive Science, Seoul National University College of Natural Science, Seoul, Korea

Introduction

Neural M-type (KCNQ/Kv7) K$^+$ channels are low threshold voltage-gated K$^+$ channels that play a crucial role in regulating excitability of neurons (Delmas and Brown 2005; Cooper and Jan 2003). Breakdown of M channels by loss of function mutations or pharmacological inhibitors leads to neuronal hyperexcitability (Schroeder et al. 1998; Delmas and Brown 2005). Indeed, linopirdine, an M channel blocker, has acute cognition-enhancing properties in some

animal experiments (Aiken et al. 1996), whereas M channel openers, such as retigabine, are currently being developed as novel antiepileptic drugs (Cooper and Jan 2003).

M currents (I_M) were originally described in sympathetic neurons (Brown and Adams 1980; Constanti and Brown 1981) and named due to their inhibition by muscarinic acetylcholine receptors. However, the signal transduction mechanism underlying muscarinic inhibition of I_M remains uncertain. Despite the fact that muscarinic inhibition of I_M was shown to be mediated by G_q-protein activation (Caulfield et al. 1994; Haley et al. 2000), typical downstream pathways of G_q such as PKC or IP_3-mediated Ca^{2+} signals were not involved in muscarinic inhibition of I_M (Beech et al. 1991; Bosma and Hille 1989; Cruzblanca et al. 1998; del Rio et al. 1999). It was shown that neuronal I_M is encoded by KCNQ family genes (Wang et al. 1998) and activities of KCNQ channels depend on phosphatidylinositol 4,5-bisphosphate (PIP_2) in the plasma membrane (Li et al. 2005; Suh et al. 2006; Zhang et al. 2003; Kim et al. 2016). Recent progress elucidated that PIP_2 modulate KCNQ2/KCNQ3 channel opening by interacting synergistically with a minimum of four cytoplasmic domains (Hernandez et al. 2008a; Choveau et al. 2018). These led to a hypothesis that depletion of PIP_2 by muscarinic stimulation is responsible for inhibition of I_M (Delmas and Brown 2005; Suh and Hille 2002).

I_M is negatively modulated by other G_q-coupled neurotransmitter receptors, such as bradykinin B_2 receptors, and purinergic P2Y receptors (Bofill-Cardona et al. 2000; Jones et al. 1995). The mechanism involved in bradykinin-induced inhibition of I_M has been particularly well characterized, and it has been shown that calmodulin activation induced by IP_3-mediated intracellular Ca^{2+} signals is responsible for I_M inhibition (Gamper et al. 2005; Gamper and Shapiro 2003). At present, it appears to be generally accepted that I_M is regulated by three modulatory pathways: PIP_2 depletion for muscarinic inhibition and second messengers, such as Ca^{2+}/CaM for bradykinin-induced inhibition (Hernandez et al. 2008b), protein kinase C (Lee et al. 2010; Kosenko et al. 2012), and post-translational modification (Kim et al. 2016; Qi et al. 2014). However, despite many studies investigating the PIP_2 depletion hypothesis for the mechanism of muscarinic inhibition of I_M (Ford et al. 2003; Suh and Hille 2002; Suh et al. 2006; Winks et al. 2005; Zhang et al. 2003), direct evidence is still lacking. In addition, since PIP_2 mobility determines the spatial and temporal profiles of PIP_2 depletion, the idea that PIP_2 depletion acts as the M_1 muscarinic signal in neurons requires that PIP_2 diffusion be slow (Cho et al. 2005). Yet, in general, PIP_2 diffuses rapidly in neurons (van Rheenen and Jalink 2002; Cho et al. 2005), making this hypothesis unlikely. The PIP_2 depletion hypothesis was supported by a result demonstrating that increasing PIP_2 concentration of sympathetic neurons by overexpressing the synthetic enzyme phosphoinositide-5 (PI-5)-kinase

can block muscarinic inhibition of I_M. Kruse and Whitten recently developed a model that describes altering M_1R surface density and PI-5-kinase activity regulating the excitability of rat SCG neurons (Kruse and Whitten 2021). However, it is not certain whether increased resting PIP_2 levels caused by overexpression of PI-5-kinase can inhibit PIP_2 depletion induced by receptor-mediated activation of PLC (Winks et al. 2005). Given that PIP_2 can modulate a variety of cellular processes, including cortical actin organization, membrane ruffling, vesicle trafficking, and gene expression (Di Paolo and De Camilli 2006), the possibility that normal signaling mechanisms involved in muscarinic inhibition of I_M are altered in excess PIP_2 cannot be excluded. To prove whether receptor-mediated inhibition is mediated by PIP_2 depletion, it is important to demonstrate that the inhibition is rescued by applying normal concentrations of exogenous PIP_2. Indeed, inhibition of GIRK channels by phenylephrine, endothelin, and PGF2α in cardiac myocytes, which were shown to be mediated via PIP_2 depletion, are completely abolished by internally perfused 10-μM PIP_2 (Cho et al. 2005, 2001). However, muscarinic inhibition of KCNQ channels was only partially reduced even by 500-μM PIP_2 (Robbins et al. 2006), which can be considered inconsistent with the PIP_2 depletion hypothesis. In the present study, we investigated the mechanism involved in muscarinic inhibition of I_M by examining various possible signaling components in rat superior cervical ganglion (SCG) sympathetic neurons and HEK cells expressing KCNQ channels.

Materials and Methods

Ethics Approval

This study was reviewed and carried out in accordance with the Institutional Animal Care and Use Committee (IACUC) at Sungkyunkwan University School of Medicine (SUSM). SUSM is an Association for Assessment and Accreditation of Laboratory Animal Care International accredited facility and abides by the Institute of Laboratory Animal Resources Guide. The animals were maintained in standard environmental conditions (25 ± 2 °C; 12/12-h dark/light cycle), were given ad libitum access to water and food, and were housed under veterinary supervision at the Laboratory Animal Research Center, SUSM. Sprague–Dawley rats were purchased from Orient Bio Inc. (Sungnam, South Korea). The authors understand the ethical principles under which The Journal of Physiology operates and the experiments comply with the animal ethics checklist described in Grundy (Grundy 2015).

Cell Culture, Transfection, and SCG Isolation

SCG neurons were cultured from 3- to 4-week-old male rats as previously described (Gamper et al. 2004). HEK293 cells were handled as previously described (Cho et al. 2006). Transfections were made using Lipofectamine 2000 reagents (Invitrogen, Carlsbad, CA) and green fluorescent protein (GFP) was used as a reporter. Plasmids encoding human KCNQ2 (GenBank accession number AF110020) and rat KCNQ3 (GenBank accession number AF091247) were kindly provided by Mark Shapiro (University of Texas Health Science Center, San Antonio, TX).

Electrophysiological Recordings

Current measurements were made with the whole-cell patch-clamp technique. Voltage clamp was performed with an EPC-8 amplifier (HEKA Instruments, Lambrecht, Germany). Filtered signals (1–2 kHz) from a patch-clamp amplifier were fed into an AD/DA converter (PCI-MIO-16E-4, National Instruments, Austin, TX), digitized at 5 kHz and stored digitally in later analysis. Electrodes were pulled from borosilicate capillaries (World Precision Instruments, Inc., Sarasota, FL) using a pipette puller (PP-83, Narishige, Tokyo) and positioned precisely with a micromanipulator (MP 225, Sutter Instrument Company, Novato, CA). The pipettes had a resistance of 2–3 MΩ when filled with pipette solution. Data were not corrected for liquid junction potential (−9 mV). For dialysis, we waited > 5 min before starting the experiment. The perfusion system was a homemade 100-µl perfusion chamber through which solution flowed continuously at 5 ml/min. All recordings were carried out at room temperature (22–24 °C).

The normal external solution for HEK293 cell and rat SCG neuron recording was as follows (in mM): 143 NaCl, 5.4 KCl, 5 HEPES, 0.5 NaH$_2$PO$_4$, 11.1 glucose, 0.5 MgCl$_2$, 1.8 CaCl$_2$, and pH 7.4 adjusted with NaOH. The pipette solution was as follows (in mM): 126 KMeSO$_4$, 14 KCl, 10 HEPES, and 3 MgCl$_2$ (pH 7.24 adjusted with KOH). 500 nM of TTX (Tocris, St. Louis, MO, Cat. #1069) and 0.1 µM of CdCl$_2$ were included in external solution to block Na$^+$ and Ca^{2+} currents.

[Ca^{2+}]$_i$ Measurement

[Ca^{2+}]$_I$, the concentration of intracellular free Ca^{2+}, was measured by loading cells with 2-µM Fura 2-acetoxymethyl ester (Fura 2-AM) (Molecular Probes, Eugene, OR) for 30 min in the recording medium. Changes in Ca^{2+} were estimated from the ratio of Fura 2 fluorescence (at 500 nm) with alternate excitation at wavelength of 340 and 380 nm, generated by a Lambda DG-4 monochromator (Sutter Instrument Company). Fura 2 ratio data (F340/380), [Ca^{2+}]$_i$, were measured at a frequency of 2 Hz. Intensity of illumination was minimized to reduce bleaching of Fura 2, while maintaining adequate levels of signal. Fura 2 images for digital analysis were generated using a system based on an Olympus IX71 microscope coupled to an image intensifier and CCD camera and were analyzed with MetaFluor software (MDS Analytical Technologies, Sunnyvale, CA).

Statistical Analysis

Results in the text and the figures are presented as mean ± S.E.M. (n = number of cells tested). Statistical analyses were performed using Student's *t* test. *P*-values of < 0.05 were considered statistically significant.

Results

Characterization of I$_M$ and Muscarinic Modulation of M Channels in SCG Neurons

I$_M$ was originally characterized as outward K$^+$ currents suppressed by muscarinic stimulation (Brown and Adams 1980) and specific blockers to inhibit I$_M$, such as linoperdine and XE991, were developed later (Aiken et al. 1996; Cooper and Jan 2003). To investigate the mechanism of muscarinic modulation of I$_M$ in rat SCG neurons, we first compared the current component inhibited by oxotremorine-M (oxo-M), a muscarinic agonist, and that inhibited by XE991. Here we used the whole-cell patch-clamp mode, a method suitable for preserving intracellular microdomains, investigating localized signaling, and directly modulating the signaling molecules driving muscarinic inhibition of M channels. To prevent the potential "run-down" of I$_M$ in the whole-cell configuration, after the pipette ruptured the membrane, we allowed I$_M$ to stabilize before tracking muscarinic inhibition. Step depolarizing pulses were applied in 10-mV steps from a holding potential of −60 mV. In Fig. 1A, representative current traces obtained in the control condition and after applying oxo-M (10 µM) or XE991 (50 µM) are shown. We obtained the current component inhibited by oxo-M (oxo-M-sensitive) and that inhibited by XE991 (XE991 sensitive) by subtracting current traces in the presence of oxo-M or XE991, respectively, from the control current traces (Fig. 1B, left panel). In Fig. 1B (*right*), current–voltage (*I-V*) relationships for total currents in control (squares), oxo-M-sensitive currents (closed circles), and XE-991-sensitive currents (open circles) were plotted. The plot shows that oxo-M-sensitive currents and XE-991-sensitive currents are similar over the voltage range tested between −60 mV and + 20 mV. Assuming that XE-991-sensitive currents represent I$_M$, I$_M$ comprises 26.49 ± 1.41% of total
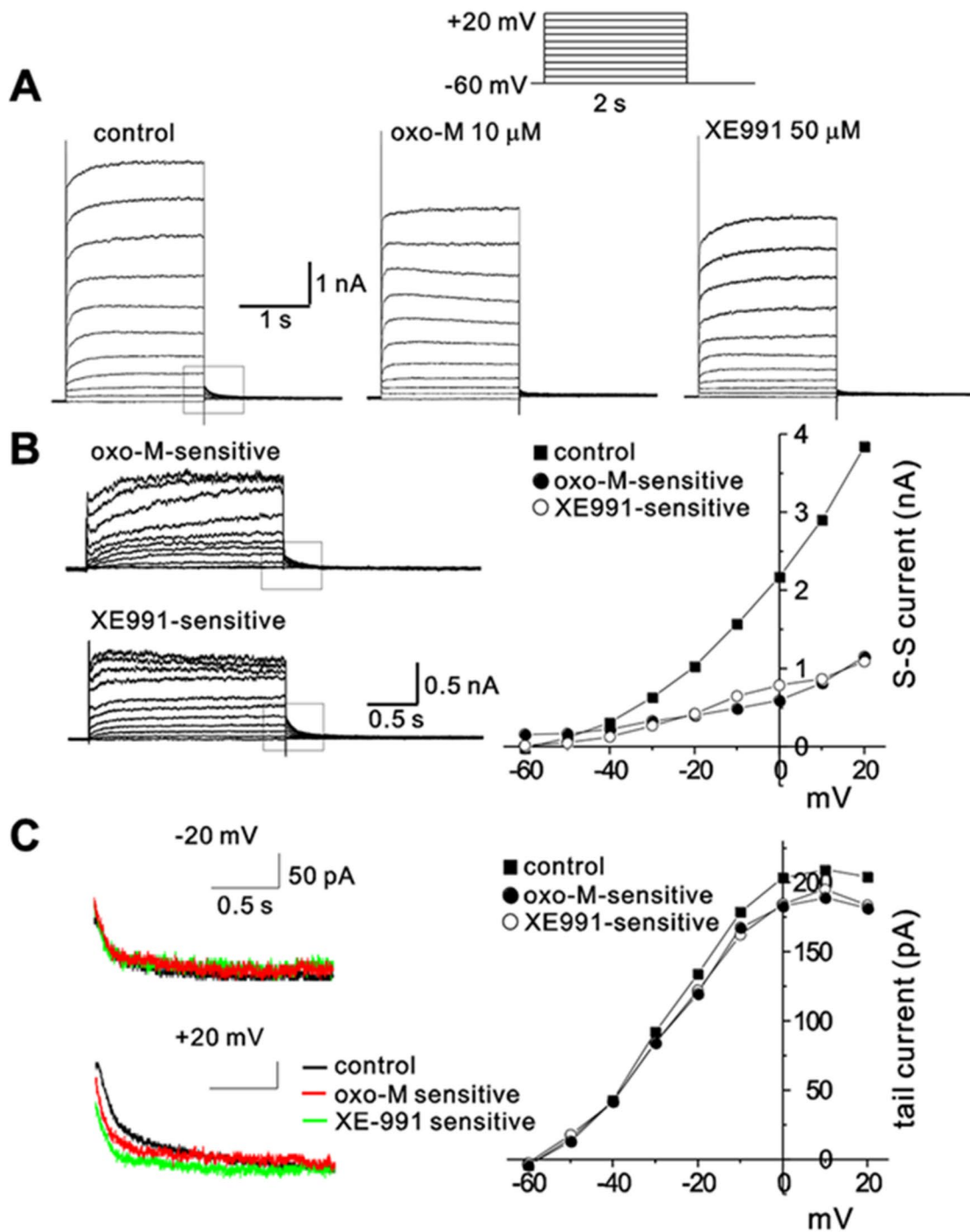
Fig. 1 Isolation of I_M from SCG neurons. **A** Families of current elicited by voltage steps from −60 mV to +20 mV, in 10-mV intervals, before (left panel) and after application of 10-μM oxo-M (middle) or 50-μM XE991 (right). Holding potential −60 mV. *Inset* shows the pulse protocol. **B** *left*, oxo-M-sensitive and XE991-sensitive currents; *right,* steady-state current–voltage (*I–V*) relationships for oxo-M-sensitive and XE991-sensitive currents shown in *left*. **C** *left*, superimposed deactivation tails for control (black), oxo-M sensitive (red), and XE991-sensitive currents (green) by hyperpolarizing steps to −60 mV from −20 mV (upper panel) or +20 mV (lower panel); *right,* *I–V* relationships for control, oxo-M-sensitive, and XE991-sensitive tail currents

outward currents at $+20$ mV and 10-μM oxo-M inhibits I_M by $79.90 \pm 13.62\%$ (at $+20$ mV, $n = 7$).

In Fig. 1C, we compared deactivation tail currents (I_{tail}) recorded upon repolarization (indicated as square boxes in Figs. 1A and B) and plotted the amplitude of I_{tail} against step depolarization voltage. To avoid contamination of capacitive currents and fast components that may not be attributable to I_M, we measured the amplitude of I_{tail} by measuring the average current level between 30 and 50 ms after repolarization and subtracting the current level at steady state. The result shows the similarity between I_{tail} of oxo-M-sensitive currents and XE-991-sensitive currents.

Furthermore, at voltage ranges up to -20 mV, I_{tail} of oxo-M-sensitive currents and XE-991-sensitive currents are almost equivalent to I_{tail} of control currents, indicating that I_{tail} corresponding to -20-mV depolarization is mostly attributable to I_M. In the present study, therefore, we regarded I_{tail} as an indication of I_M.

The concentration-dependent effects of oxo-M to inhibit I_M were tested, while changes of I_{tail} were monitored in 5-s intervals by applying a hyperpolarizing pulse to -60 (or -55) mV for 1.5 s from the holding potential of -20 mV. Extent of inhibition induced by 1-μM and 10-μM oxo-M were $42.54 \pm 3.51\%$ (n = 12) and $84.13 \pm 7.34\%$ (n = 16), respectively (Fig. 2C).
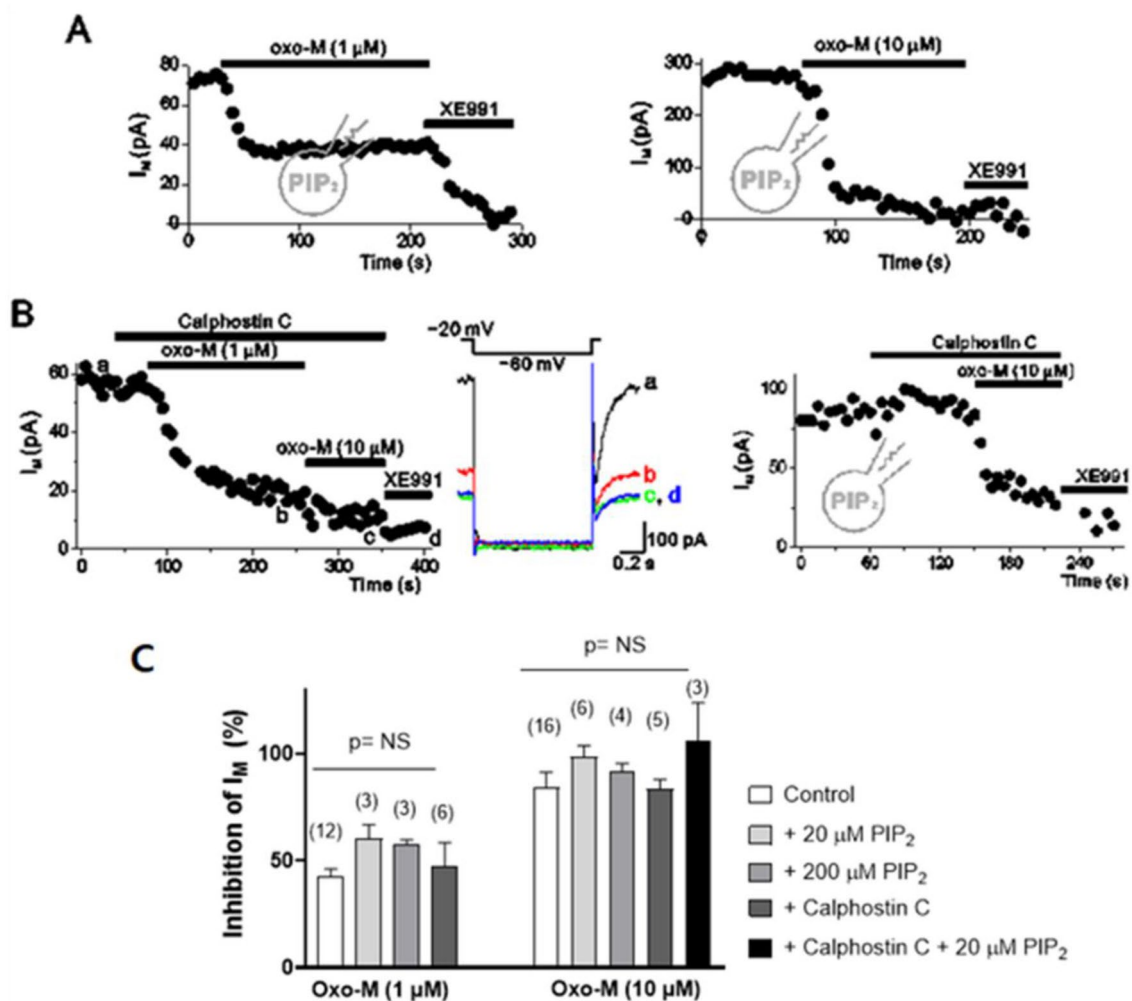

Fig. 2 Muscarinic inhibition of I_M was not blocked either by supply of PIP$_2$ or by PKC inhibitor. The current amplitudes were measured as the deactivation tail current induced by 1-s hyperpolarizing steps to -60 mV from a holding potential of -20 mV at 5-s intervals. **A** The effects of 1-μM oxo-M (*left*) or 10-μM oxo-M (*right*) on I_M in cells which were patched with 20-μM diC8-PIP$_2$. **B** Time course of I_M amplitude during cumulatively increasing concentration of oxo-M indicated. Neurons were pretreated by 1-μM calphostin C without (*left*) and with (*right*) 20-μM diC8-PIP$_2$ in the patch pipet. *Inset* shows the pulse protocol and representative current traces of *left* panel. **C** Summary of the percent inhibitions of I_M by oxo-M in control conditions or in cells applied with various concentrations of PIP$_2$ or calphostin C. Values are expressed as means $\pm$ S.E.M. NS, not significant ($p > 0.05$)

Re-examination of the Current Hypothesis: PIP$_2$ Depletion and PKC Activation

PIP$_2$ depletion and PKC activation have been considered to be the most likely candidates involved in muscarinic inhibition of I$_M$ (Delmas and Brown 2005). However, previous studies have found that muscarinic inhibition of I$_M$ was not fully blocked by application of exogenous PIP$_2$ or PKC inhibitors (Brown and Yu 2000; Ford et al. 2003; Hoshi et al. 2003; Robbins et al. 2006; Shapiro et al. 2000). We confirmed that exogenous PIP$_2$ (up to 200 μM) had little effect on muscarinic inhibition of I$_M$ (Fig. 2A). Consistent with the data from sympathetic neurons, in HEK293 cells expressing KCNQ2/KCNQ3 channels and M1 muscarinic receptors, application of PIP$_2$ did not block the effect of oxo-M on I$_M$ (Yoon 2010). To apply PIP$_2$ into cells, diC8-PIP$_2$ was added to the pipette solution, and the conventional whole-cell mode was accomplished by rupturing membranes after a giga-seal was made. We have recently shown that application of diC8-PIP$_2$ disrupts M channel regulation induced by the altered channel's affinity for PIP$_2$ (Lee et al. 2010), suggesting that exogenous PIP$_2$ is effectively delivered to the plasma membrane and available to M channels. We also confirmed that calphostin C, a highly specific PKC inhibitor, did not affect muscarinic inhibition of I$_M$ (Fig. 2B). Summarized data are shown in Fig. 2C. In addition, a higher dose of calphostin C (up to 10 μM) and two other PKC inhibitors, 1-μM chelerythrine and 100-nM bisindolylmaleimide I, were tested and neither affected oxo-M-induced M current modulation (SI 1).

We then hypothesized that muscarinic inhibition of I$_M$ uses multiple signaling pathways such that inhibition can only be blocked when multiple pathways are simultaneously suppressed. To test this hypothesis, both PIP$_2$ depletion and PKC activation were prevented with exogenous PIP$_2$ (20 μM) and calphostin C (1 μM). In the presence of 20-μM PIP$_2$ and calphostin C, however, 10-μM oxo-M was still capable of inhibiting I$_M$ (Fig. 2B and C).

Looking for New Possibilities

Since we did not find evidence that messengers downstream of the Gα_q pathway mediate muscarinic inhibition of I$_M$, we searched for other possibilities. It is well known that the G$_{\beta\gamma}$ dimer mediates voltage-dependent modulation of N-type Ca^{2+} channels through numerous neurotransmitters, including noradrenaline, acetylcholine, and dynorphin (Herlitze et al. 1996; Ikeda 1996; Tsien et al. 1988). We tested the involvement of the G$_{\beta\gamma}$ subunit in oxo-M-induced I$_M$ modulation using HEK cells transfected with G$_\alpha$-transducin (G$_\alpha$TD) together with KCNQ2, KCNQ3, and M$_1$ muscarinic receptors. G$_\alpha$TD is a G$_\alpha$ subunit which predominantly attains the GDP-bound state when overexpressed in SCG neurons and buffers G$_{\beta\gamma}$ (Kammermeier and Ikeda 1999). As shown in Fig. 3A, expression of G$_\alpha$TD did not affect muscarinic inhibition of the KCNQ current by 1-μM oxo-M ($87.84 \pm 4.02\%$ ($n = 4$) in controls or $89.77 \pm 7.74\%$ ($n = 5$) in G$_\alpha$TD-expressed cells, $p > 0.05$). In addition, scavenging G$_{\beta\gamma}$ subunits with intracellular anti-G$_{\beta\gamma}$ antibody in SCG neurons was also tested. In the presence of anti-G$_{\beta\gamma}$ antibody, 10-μM oxo-M-induced inhibition of M current was not different from control conditions. (Fig. 3B) These data implicate that G$_{\beta\gamma}$ subunits do not have a critical role in muscarinic inhibition of I$_M$.

Recently, it was reported that receptor activation regulates channel activity by affecting the surface expression of channel proteins (Chung et al. 2009). Because KCNQ channels are known to be targets of trafficking, i.e., insertion into and removal from the plasma membrane (Etxeberria et al. 2008; Schuetz et al. 2008), we tested the possibility that KCNQ channel trafficking is involved in muscarinic inhibition of I$_M$. However, a block of protein trafficking with 50-μM blebbistatin, a cell-permeable inhibitor of class-II myosins, did not affect muscarinic inhibition of I$_M$ (SI 2). In addition, pretreatment of a protein trafficking inhibitory cocktail including chloroquin (100 μM), monensin (100 μM), and nocodazole (20 μM) had no effect on muscarinic modulation of I$_M$ (data not shown), suggesting that KCNQ channel trafficking did not contribute to the regulation of I$_M$ by M$_1$ muscarinic receptors.

Revisiting Ca^{2+}-Dependent Hypothesis

Recently, the role of Ca^{2+} signaling in I$_M$ inhibition was well established for I$_M$ inhibition by bradykinin (Gamper et al. 2005; Gamper and Shapiro 2003) or by P2Y receptor stimulation (Zaika et al. 2007), in which CaM was shown to be responsible. However, inhibition of CaM activation using dominant-negative CaM that cannot bind Ca^{2+} (Geiser et al. 1991) did not affect muscarinic inhibition of I$_M$ (Gamper and Shapiro 2003; Zaika et al. 2007), leading to the conclusion that Ca^{2+} signaling is not involved in muscarinic inhibition of I$_M$. This conclusion was supported by the observation that in SCG neurons, oxo-M did not induce Ca^{2+} transients as robustly as bradykinin did (Cruzblanca et al. 1998; del Rio et al. 1999). In early experiments, however, muscarinic inhibition of I$_M$ was shown to be suppressed when intracellular Ca^{2+} was heavily buffered (Beech et al. 1991). Further, Shapiro et al. (Shapiro et al. 2000) reported that oxo-M-induced Ca^{2+} transients are blocked by thapsigargin. Taken together, these findings implicate Ca^{2+} signaling in muscarinic receptor stimulation. Thus, we re-examined the roles of Ca^{2+} signaling in muscarinic inhibition of I$_M$ inhibition.

First, we examined whether oxo-M could induce Ca^{2+} transients in SCG neurons and whether oxo-M-induced Ca^{2+} transients would be significantly smaller than
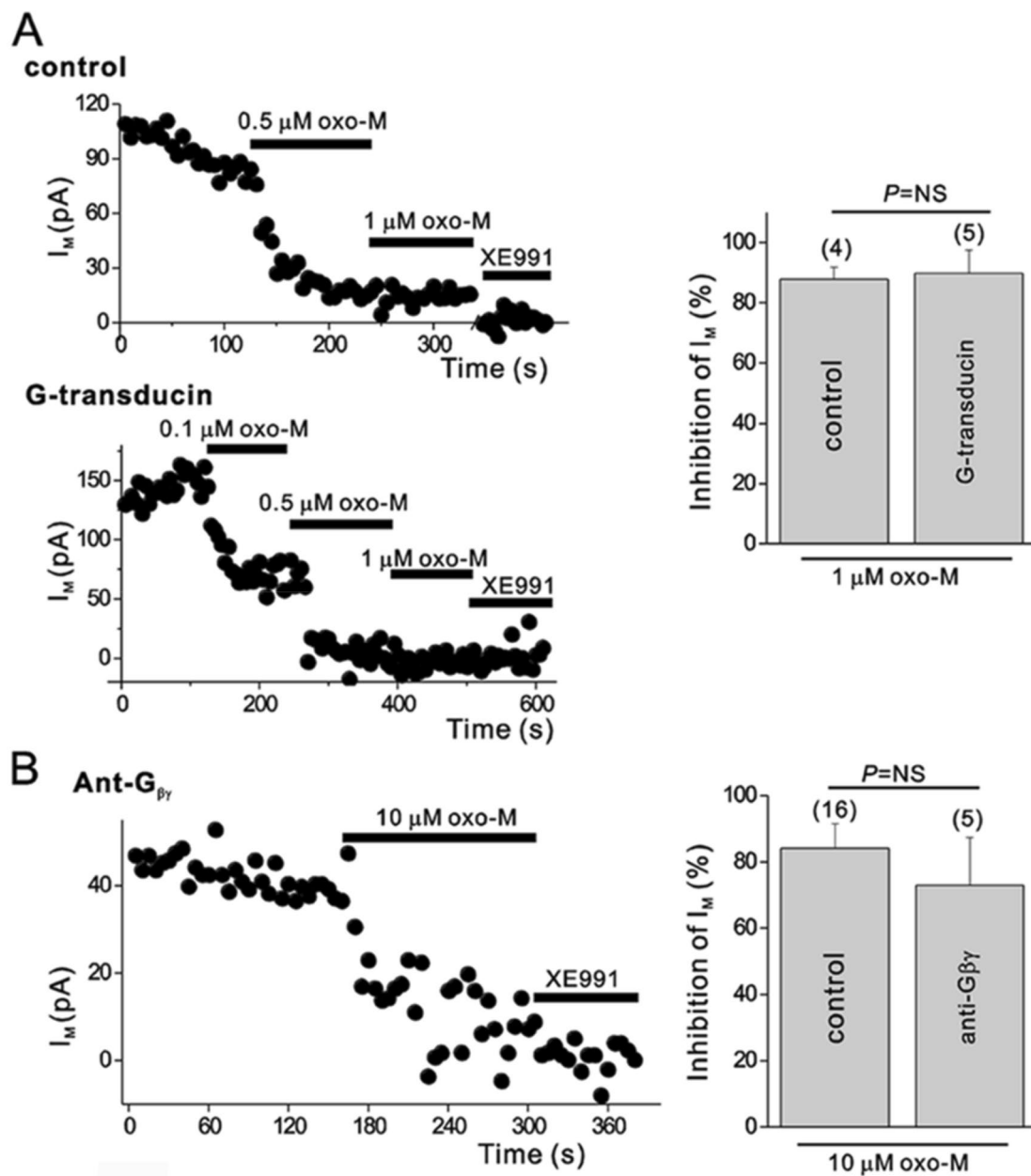
Fig. 3 $G_{\beta\gamma}$-buffering proteins did not affect muscarinic modulation of I_M. **A** *Left*, time course of I_M amplitude during cumulatively increasing concentrations of oxo-M in control HEK cells expressing KCNQ2/3 channels and M_1 muscarinic receptors (upper panel) and cells expressing channels and M1Rs plus $G\alpha$-transducin (lower panel). *Right*, summary of the percent inhibitions of I_M by oxo-M, collected as in *left*. **B** *Left*, time course of I_M in SCG neurons loaded with anti-$G_{\beta\gamma}$ antibody. *Right*, summarized data for the effects of anti-$G_{\beta\gamma}$ antibody on muscarinic inhibition of I_M. Values are expressed as means ± S.E.M

bradykinin-induced Ca^{2+} transients, as previously described (Cruzblanca et al. 1998; del Rio et al. 1999). $[Ca^{2+}]_i$ was measured in SCG neurons using Fura 2-AM. As shown in Fig. 4, 10-μM oxo-M did induce Ca^{2+} transients in all SCG neurons tested though there was large cell-to-cell variation. On average, oxo-M-induced Ca^{2+} transients were not different from bradykinin-induced Ca^{2+} transients (Fig. 4). The

peak amplitude of Ca^{2+} transient induced by oxo-M was similar to that induced by bradykinin. Paired *t* test confirmed that the effects of oxo-M on intracellular Ca^{2+} concentration were not significantly different from those of bradykinin in the same neurons ($n = 3$, $p > 0.05$). These results imply that the Ca^{2+}-releasing powers of oxo-M and bradykinin are not significantly different.

Fig. 4 Muscarinic stimulation raises $[Ca^{2+}]_i$ in rat SCG neurons. SCG neurons were loaded with 2-μM Fura 2-AM for Ca^{2+} measurements. The F340/F380 ratio was used to estimate $[Ca^{2+}]_i$. F340/F380 ratio (F´) changes in oxo-M or bradykinin-stimulated cells was summarized. Open circles indicate means ± S.E.M. *Inset* shows two representative $[Ca^{2+}]_i$ recordings of each group
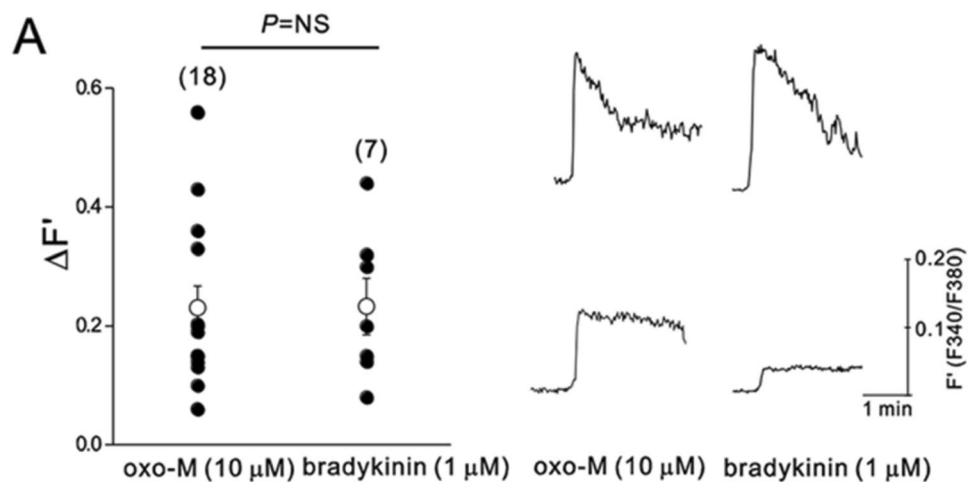
Since muscarinic receptor stimulation elicited an increase of $[Ca^{2+}]_i$, we tested whether Ca^{2+} mediates muscarinic modulation of I_M using 20-mM BAPTA. When the pipette solution contained 20-mM BAPTA, oxo-M minimally affected I_M (Fig. 5Aa). Superimposed deactivation tail currents showed that in a cell dialyzed with 20-mM BAPTA, I_M after 5 min oxo-M treatment was almost overlapped with that in controls. To rule out the possibility that I_M itself was reduced by 20-mM BAPTA, we obtained the steady-state current–voltage relationships for oxo-M-sensitive currents and XE-991-sensitive currents in BAPTA-loaded cells, using the same protocol as in Fig. 1. Figure 5Ac demonstrates the proportion of XE991-sensitive currents to total steady-state currents in 20-mM BAPTA-loaded cells was not reduced compared to that in 0.1-mM EGTA ($52.40 \pm 2.46\%$ [$n=19$] *vs.* control: $26.49 \pm 1.41\%$ [$n=7$] at $+20$ mV). The oxo-M-induced inhibition of I_M was determined as a proportion of oxo-M-sensitive currents to XE991-sensitive currents at $+20$ mV as in Fig. 1 and was $22.21 \pm 3.94\%$ ($n=19$, Fig. 5Ac), which was significantly smaller than that in controls ($79.90 \pm 13.62\%$ ($n=7$), $p<0.01$). We then tested whether the effect of BAPTA on suppressing muscarinic inhibition of I_M could be attributed to inhibiting local Ca^{2+} signals. To do this, we tested the effect of EGTA on muscarinic inhibition of I_M. BAPTA is a fast Ca^{2+} buffer that effectively buffers all types of Ca^{2+} signals, whereas EGTA is a slow Ca^{2+} buffer that selectively spares local Ca^{2+} signals (Neher 1998). With 20-mM EGTA, muscarinic receptors were still able to inhibit M currents (Fig. 5Ba). The oxo-M-induced inhibition of I_M was calculated as a proportion of oxo-M-sensitive currents to XE991-sensitive currents at $+20$ mV and was $103.05 \pm 11.60\%$ ($n=5$, Fig. 5Bc), which was not significantly different from that of control conditions ($p>0.05$). We confirmed that proportions of I_M to total outward currents in the presence of 20-mM EGTA ($49.60 \pm 3.48\%$ [$n=4$]) at $+20$ mV) were similar to those in the presence of 20-mM BAPTA ($52.40 \pm 2.46\%$ [$n=19$]).

Next, we directly examined the effect of $[Ca^{2+}]_i$ on M currents in SCG neurons. We perfused cells with a bathing solution containing 10-μM ionomycin, a Ca^{2+} ionophore, and 10-mM $CaCl_2$ to raise $[Ca^{2+}]_i$. We found that as $[Ca^{2+}]_i$ increased, the M current amplitude declined in parallel (SI 3). This is consistent with previous data showing the sensitivity of KCNQ2/KCNQ3 channels to $[Ca^{2+}]_i$ (Delmas and Brown 2005; Gamper and Shapiro 2003; Kosenko and Hoshi 2013). Taken together, these data suggest that Ca^{2+} signals play a critical role in M_1 muscarinic receptor-mediated regulation of M channels. The differential effects of EGTA and BAPTA imply that M channels are very close to Ca^{2+} sources and are regulated by local Ca^{2+} signals.
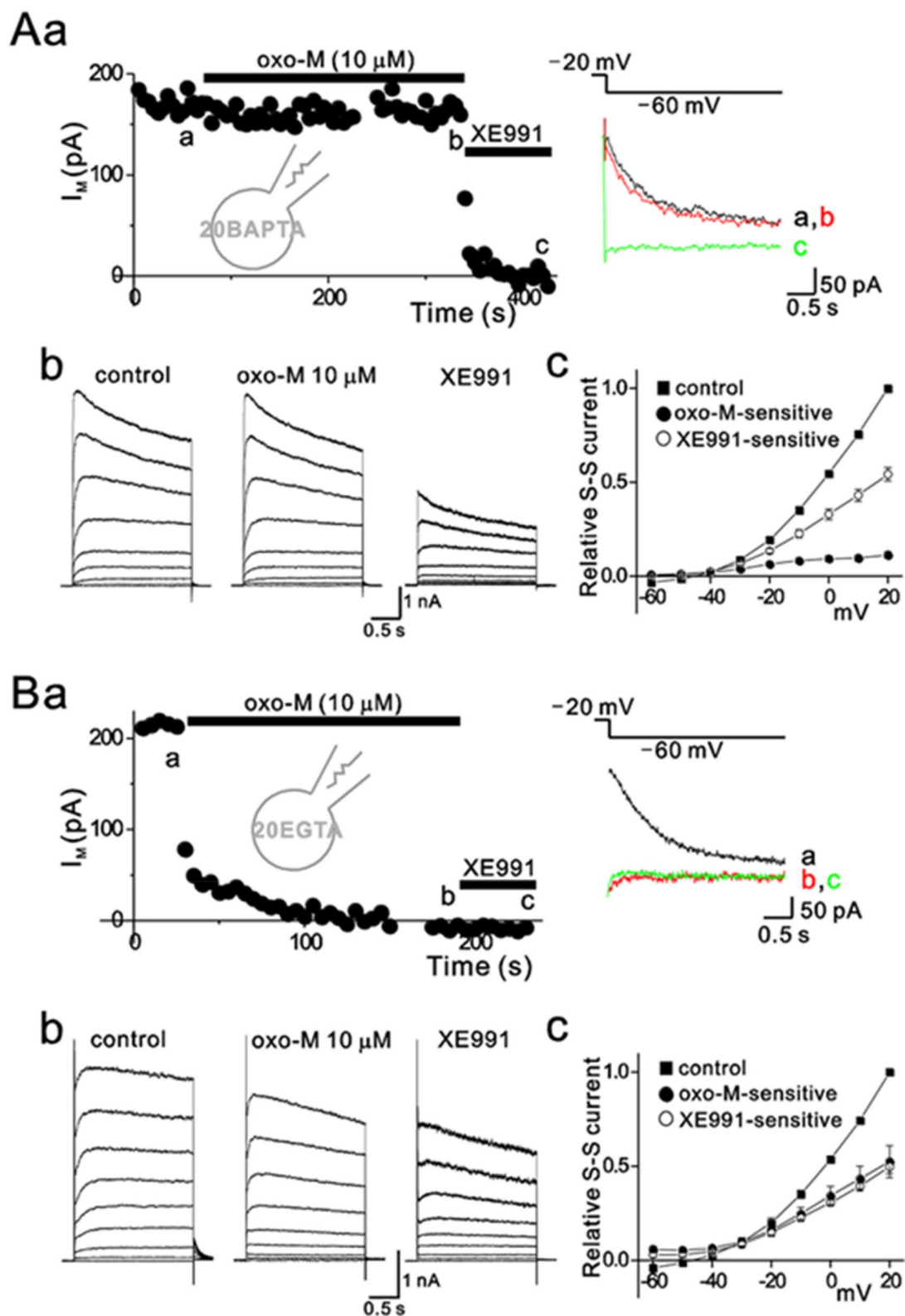
Discussion

We have demonstrated that muscarinic inhibition of I_M in rat SCG neurons is significantly suppressed by 20-mM BAPTA in pipette solutions (Fig. 5). In fact, similar findings were observed in earlier studies (Beech et al. 1991; Kirkwood et al. 1991). However, Ca^{2+} was not regarded as a candidate for couple muscarinic receptor activation to M channel inhibition, because oxo-M failed to increase the intracellular Ca^{2+} concentration in SCG neurons (Beech et al. 1991; del Rio et al. 1999). The current understanding of the distinction between muscarinic receptor-induced inhibition of I_M and bradykinin-induced inhibition of I_M relies, at least in part, on the inability of oxo-M to induce Ca^{2+} increase (Delmas and Brown 2005). However, some controversial reports stated that oxo-M induces Ca^{2+} increase in acutely dissociated rat SCG neurons (del Rio et al. 1999; Cruzblanca et al. 1998) and tsA-201 cells (Falkenburger et al. 2013). Furthermore, oxo-M was invariably shown to induce Ca^{2+} mobilization in other parts of the brain (Irving and Collingridge 1998; Seymour-Laurent and Barish 1995), and oxo-M-induced effects, such as GIRK channel inhibition, were shown to be mediated

by Ca^{2+}-dependent mechanisms (Sohn et al. 2007). Other reports exploring the PIP_2 depletion hypothesis showed that M current could be inhibited by muscarinic receptors in neurons overexpressing the neuronal calcium sensor, NCS-1 (Winks et al. 2005). NCS-1 up-regulates PI-4-kinase, which catalyzes the first step in PIP_2 synthesis from PI and requires Ca^{2+} to be activated (Koizumi et al. 2002; Rajeb-hosale et al. 2003; Zhao et al. 2001; Taverna et al. 2002; Burgoyne and Weiss 2001). In neurons overexpressing NCS-1, Winks et al. reported that M current inhibition by oxo-M was conserved, while the inhibitory effect of bradykinin was reduced (Winks et al. 2005). They claimed that oxo-M does not evoke enough Ca^{2+} release to activate NCS-1 for replenishing PIP_2 hydrolyzed by muscarinic stimulation. However, others reported similar basal Ca^{2+} levels, ~ 100 nM, in PC12 cells and SCG neurons, which are enough to activate NCS-1 in PC12 cells (Cruzblanca et al. 1998; Delmas et al. 2002; Meijer et al. 2014; Koizumi et al. 2002; Rajebhosale et al. 2003; Taverna et al. 2002). In this case, under basal conditions during muscarinic receptor activation, NCS-1 could compensate for PIP_2 consumption by PLC. If PIP_2 depletion hypothesis is true, in cells overexpressing NCS-1, oxo-M is unlikely to inhibit M current because NCS-1 replenishes PIP_2 but supporting our hypothesis that PIP_2 depletion is not the primary mechanism.

In the present study, we re-examined whether the inability of oxo-M to induce Ca^{2+} mobilization is a consistent finding. Surprisingly, we found that muscarinic receptor stimulation by oxo-M is capable of increasing intracellular Ca^{2+} concentration in rat sympathetic neurons. We noted that the cell-to-cell variation of the amplitude of Ca^{2+} transients was quite large; thus, in some cells, Ca^{2+} transients induced by oxo-M were small, which was similar to a previous report (Delmas and Brown 2002). However, this was also the case for B2R-induced Ca^{2+} transients (Fig. 4). Thus, we conclude that the current understanding of dual modulatory pathways for M channel regulation based on different Ca^{2+} mobilization powers, the ability to evoke changes of $[Ca^{2+}]_i$, needs to be re-examined. We do not know the reason for the discrepancy of Ca^{2+} mobilization power of oxo-M among different studies, but differences in receptor density (Dickson et al. 2013; Falkenburger et al. 2013; Kruse and Whitten 2021), signaling microdomains that modify the efficacy of IP_3 to open its receptor (Zaika et al. 2011), or experimental conditions may be involved. Previous studies used voltage-clamped neurons with Fura 2 in pipette solutions and held the membrane potential near or below −60 mV during Ca^{2+} measurements (Beech et al. 1991; del Rio et al. 1999; Falkenburger et al. 2013; Dickson et al. 2013), whereas we used intact sympathetic neurons with Fura 2-AM. If Ca^{2+} entry through the voltage-dependent ion channels contributed to the oxo-M-induced $[Ca^{2+}]_i$ rises, this pathway might have been blocked by clamping the membrane potential

hyperpolarized to −60 mV or below. The fact that removal of external Ca^{2+} prevented the rise of $[Ca^{2+}]_i$ by muscarinic receptor stimulation may support this possibility (Foucart et al. 1995).

In fact, it was also observed in earlier studies that high concentrations of Ca^{2+} chelator (20-mM BAPTA) can suppress muscarinic inhibition of I_M (Beech et al. 1991; Kirkwood et al. 1991). However, when 10-mM Ca^{2+} was added to 20-mM BAPTA-containing pipette solutions to increase free Ca^{2+} concentration from 12 to 143 nM, oxo-M was still capable of inhibiting I_M (Beech et al. 1991; Cruzblanca et al. 1998). These results were interpreted to mean that the effect of BAPTA to inhibit a muscarinic effect on I_M was attributable to lowering of resting $[Ca^{2+}]_i$ rather than inhibiting the rise of $[Ca^{2+}]_i$ by muscarinic stimulation (Beech et al. 1991). This interpretation was based on the assumption that adding 10-mM Ca^{2+} to 20-mM BAPTA-containing solution increases free Ca^{2+} concentration without affecting Ca^{2+} buffering power during the event of rising $[Ca^{2+}]$. That is not the case, but Ca^{2+} buffering power is compromised because BAPTA is occupied by the added Ca^{2+}, resulting in reduction of free BAPTA that is capable of buffering Ca^{2+} rise. Therefore, these results and our results may present evidence that Ca^{2+} signals that mediate muscarinic inhibition of I_M are only suppressed by a very high concentration of BAPTA. The requirement of high concentrations of BAPTA may imply two possibilities: muscarinic inhibition of I_M somehow requires minimum resting Ca^{2+}, as was suggested previously (Beech et al. 1991), or muscarinic inhibition of I_M is mediated by local Ca^{2+} signals that can be suppressed by high concentrations of fast Ca^{2+} buffer, BAPTA. To distinguish these two possibilities, we tested 20-mM EGTA, which has similar equilibrium affinities for binding Ca^{2+} with BAPTA, but its Ca^{2+}-binding rate is too slow to suppress dynamic Ca^{2+} rises. Since it is expected that resting Ca^{2+} concentrations should be lowered to the same extent by EGTA as it is by BAPTA, differences in the ability of BAPTA and EGTA to block Ca^{2+}-triggered responses can be regarded to represent the involvement of local Ca^{2+} signals. Indeed, we found that muscarinic inhibition of I_M was potently blocked by BAPTA but completely insensitive to EGTA (Fig. 5), implying that the spatial proximity between the Ca^{2+} source of oxo-M-induced Ca^{2+} rise and Ca^{2+}-sensitive target proteins that mediate I_M inhibition is so close that the coupling can only be blocked by very high concentrations of fast Ca^{2+} buffer. We calculated the length constant of Ca^{2+} microdomain in the presence of either BAPTA or EGTA, λ, which represents the mean distance that a Ca^{2+} ion diffuses before it is captured by a buffer molecule (Fig. 6). According to equation (7) by Neher (Neher 1998), $\lambda = \sqrt{(D_{Ca}/k_{on} [B]^o}$ (k_{on} and $[B]^o$ representing the rate constant of Ca^{2+} binding to the buffer and the concentration of free buffer, respectively). We referred

◄**Fig. 5** Intracellular BAPTA, but not EGTA suppresses muscarinic modulation of I_M. The current inhibition induced by 10-μM oxo-M were measured in cells dialyzed with 20-mM BAPTA (**A**) or 20-mM EGTA (**B**). *a*, time course of tail current amplitude induced by the pulse protocol as shown in the inset. *Right*, superimposed deactivation tail currents before (black) or after application of oxo-M or XE991. *b*, families of current elicited by voltage steps from −60 mV to +20 mV, in 10-mV intervals, before (left panel) and after application of 10-μM oxo-M (middle panel) or XE991 (right panel) in a cell shown in *a*. *c*, pooled data for normalized oxo-M-sensitive (closed circles) and XE991-sensitive steady currents (open circles) to control steady-state currents at +20 mV, collected as in *b*

of 20-mM BAPTA and 20-mM EGTA, respectively. Thus, our results imply that M channels are localized in the vicinity of the muscarinic receptor sensitive Ca^{2+} source within 60 nm, but away from this source at more than 5 nm. To prove this model, it is necessary to identify the Ca^{2+} source and Ca^{2+}-sensitive target proteins involved in I_M inhibition. Further studies will be required to clarify this issue.

In addition, our results showed that muscarinic inhibition of M channel was not attenuated by blocking PIP_2 depletion with supply of PIP_2 (up to 200 μM), or by blocking PKC activation with a specific blocker, calphostin C, or by blocking both PIP_2 and PKC pathways. As other potential signaling pathways may have been involved, we examined whether $G_{\beta\gamma}$ subunits of G protein or trafficking of channel proteins were involved in muscarinic inhibition of I_M. The results showed that neither seemed to have a critical role.

Our data demonstrate that PIP_2 depletion is not the 'principal' contributor to the inhibition of I_M by muscarinic signaling, in contrast to the PIP_2 depletion hypothesis for muscarinic action. Clearly, KCNQ channels are PIP_2 sensitive: they are directly activated by exogenous PIP_2 (Zhang et al. 2003). However, two distinct questions must be answered to evaluate the role of PIP_2 signals. The first is whether PIP_2 functions as a regulator of channel activity and a second, distinct question is whether PIP_2 signals play a role in M channel modulation by muscarinic receptors. The PIP_2 depletion hypothesis is based on a number of experiments focusing on the first question. For example, selective depletion of PIP_2 using an engineered chemical dimerization system almost completely suppressed the current, whereas PIP_2 directly applied to excised patches augmented the current (Suh et al. 2006; Zhang et al. 2003). These data, however, cannot rule out the possibility that during muscarinic signaling, PIP_2 depletion plays no role in decreasing current amplitudes. To determine the role of PIP_2 in receptor-mediated regulation of ion channels, specific experiments testing the role of PIP_2 in receptor-induced channel modulation are needed. To do this, we and others applied exogenous PIP_2 into neurons during G_qPCRs signaling. This experimental protocol was used to confirm the role of PIP_2 depletion in G_qPCR-mediated GIRK channel regulation (Cho et al. 2005, 2001; Meyer

et al. 2001). As opposed to PIP_2-mediated GIRK channel regulation, muscarinic inhibition of KCNQ channels was not suppressed by PIP_2 (up to 200 μM, Fig. 2) and only partially reduced even by 500-μM PIP_2 (Robbins et al. 2006). These results underscore the notion that PIP_2 depletion might play only a small role in muscarinic inhibition of I_M. Another piece of evidence in favor of the PIP_2 model is that the dynamics and extent of channel inhibition by muscarinic receptors showed a close correlation to the translocation of the PH-GFP construct that provided a measure of overall PIP_2 hydrolysis (Hernandez et al. 2008b; Horowitz et al. 2005). However, the dynamics of PIP_2 hydrolysis does not necessarily correlate to the dynamics of PIP_2 depletion, especially in the proximity of a given ion channel. Since no method is available to measure changes in local concentrations of PIP_2, we developed a two-dimensional diffusion model to estimate them. Using this model, we found that the key to determining the spatial and temporal profiles of PIP_2 depletion is PIP_2 mobility (Cho et al. 2005), in that a profound PIP_2 depletion restricted to the microdomain adjacent to PLC occurs only when PIP_2 mobility is low. However, in general, diffusion constants for PIP_2 in neurons are not low (~ 0.5–2 μm²/s, (van Rheenen and Jalink 2002; Cho et al. 2005)) and there is no evidence that the physical properties of PIP_2 in SCG neurons are dissimilar from those of PIP_2 in other neurons. When PIP_2 is diffusible, the PIP_2 depletion induced by PLC activation is readily attenuated by diffusion, so that the resulting changes become slower and smaller (Cho et al. 2005; Cui et al. 2010). This is in contrast to the rapid and profound I_M inhibition observed during muscarinic stimulation. Support for the PIP_2 model also comes from the fact that the recovery from inhibition requires cytoplasmic ATP and is delayed by inhibition of the PI-4-kinase, which replenishes PIP_2 (Ford et al. 2003; Suh and Hille 2002). However, although recovery from inhibition requires resynthesis of PIP_2, whether the process of inhibition itself results directly from PIP_2 breakdown is unclear. It must be noted that for GIRK channels in HEK cells, the recovery from receptor-induced inhibition depends primarily on PIP_2 regeneration but receptor-induced inhibition results primarily from the change in the channel's affinity for PIP_2 by other signaling molecules (Brown et al. 2005). Furthermore, as mentioned earlier, although muscarinic inhibition of I_M is reduced by over-expressing the synthetic enzyme PI-5-kinase (Winks et al. 2005), whether muscarinic receptor signaling no longer functions in cells with increased resting PIP_2 level caused by overexpression of PI-5-Kinase needs to be tested and resolved.

Reportedly, Ca^{2+} elevation does not require as much G_qPCR stimulation or local receptor density as does PIP_2 depletion or M channel inhibition (Falkenburger et al.
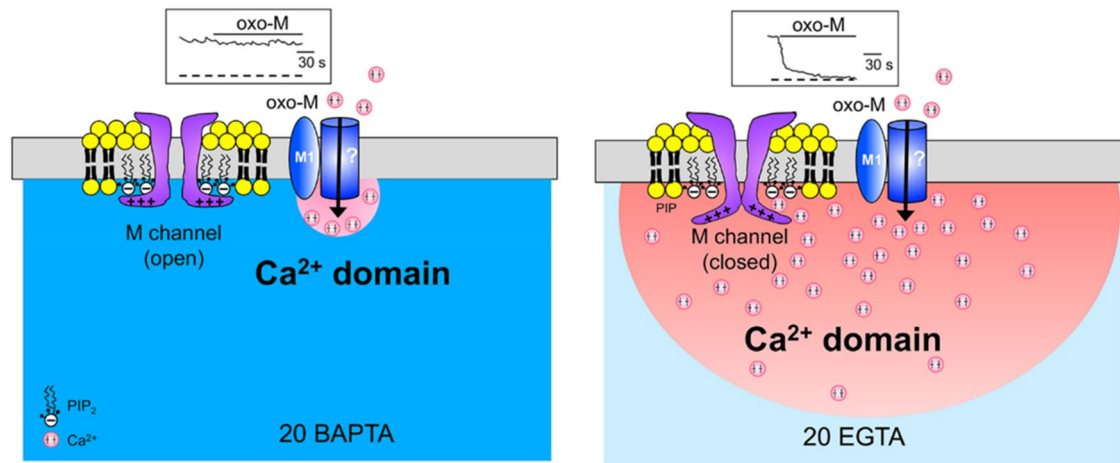
Fig. 6 Model for Ca^{2+} microdomains for muscarinic modulation of I_M in SCG neurons. The length constant of Ca^{2+} microdomains associated with individual M1 muscarinic receptors (M1) is calculated to be ~5 nm and 60 nm in the presence of 20-mM BAPTA (*left*) and 20-mM EGTA (*right*), respectively. Ca^{2+} rises in response to muscarinic stimulation can lead to weakening channel–PIP_2 interaction, resulting in the decrease of M currents

2013; Dickson et al. 2013; Kruse and Whitten 2021). Thus, Ca^{2+} signaling sensitizes SCG neurons to M_1R activation, allowing I_M inhibition even when M_1R is at low receptor density or under minimal muscarinic acetylcholine stimulation.

The results of our study do not exclude or support the possibility that PIP_2 depletion and Ca^{2+} elevation might occur simultaneously in response to muscarinic stimulation; and this could enhance the inhibitory effect. However, we do show that use of exogenous Ca^{2+} buffer to inhibit Ca^{2+} rises could block muscarinic inhibition, whereas exogenously restoring PIP_2 levels could not, suggesting Ca^{2+} elevation, not PIP_2 depletion, is the principal driver of muscarinic inhibition of M currents.

Declarations

Conflict of interest The authors declare that they have no conflict of interest.

Ethical Approval This study was reviewed and carried out in accordance with the Institutional Animal Care and Use Committee (IACUC) at Sungkyunkwan University School of Medicine (SUSM).

Consent to participate Not applicable.

Consent to publish Not applicable.

References

Aiken SP, Zaczek R, Brown BS (1996) Pharmacology of the neurotransmitter release enhancer linopirdine (DuP 996), and insights into its mechanism of action. Adv Pharmacol 35:349–384. https://doi.org/10.1016/s1054-3589(08)60281-1

Allbritton NL, Meyer T, Stryer L (1992) Range of messenger action of calcium ion and inositol 1,4,5-trisphosphate. Science 258(5089):1812–1815. https://doi.org/10.1126/science.1465619

Beech DJ, Bernheim L, Mathie A, Hille B (1991) Intracellular Ca2+ buffers disrupt muscarinic suppression of Ca2+ current and M current in rat sympathetic neurons. Proc Natl Acad Sci USA 88(2):652–656. https://doi.org/10.1073/pnas.88.2.652

Bofill-Cardona E, Vartian N, Nanoff C, Freissmuth M, Boehm S (2000) Two different signaling mechanisms involved in the excitation of rat sympathetic neurons by uridine nucleotides. Mol Pharmacol 57(6):1165–1172

Bosma MM, Hille B (1989) Protein kinase C is not necessary for peptide-induced suppression of M current or for desensitization of the peptide receptors. Proc Natl Acad Sci USA 86(8):2943–2947. https://doi.org/10.1073/pnas.86.8.2943

Brown DA, Adams PR (1980) Muscarinic suppression of a novel voltage-sensitive K+ current in a vertebrate neurone. Nature 283(5748):673–676. https://doi.org/10.1038/283673a0

Brown BS, Yu SP (2000) Modulation and genetic identification of the M channel. Prog Biophys Mol Biol 73(2–4):135–166. https://doi.org/10.1016/s0079-6107(00)00004-3

Brown SG, Thomas A, Dekker LV, Tinker A, Leaney JL (2005) PKC-delta sensitizes Kir3.1/3.2 channels to changes in membrane phospholipid levels after M3 receptor activation in HEK-293 cells. Am J Physiol Cell Physiol 289(3):C543-556. https://doi.org/10.1152/ajpcell.00025.2005

Burgoyne RD, Weiss JL (2001) The neuronal calcium sensor family of Ca2+-binding proteins. Biochem J 353(Pt 1):1–12

Caulfield MP, Jones S, Vallis Y, Buckley NJ, Kim GD, Milligan G, Brown DA (1994) Muscarinic M-current inhibition via G alpha q/11 and alpha-adrenoceptor inhibition of Ca2+ current via G alpha o in rat sympathetic neurones. J Physiol 477(Pt 3):415–422. https://doi.org/10.1113/jphysiol.1994.sp020203

Cho H, Nam GB, Lee SH, Earm YE, Ho WK (2001) Phosphatidylinositol 4,5-bisphosphate is acting as a signal molecule in alpha(1)-adrenergic pathway via the modulation of acetylcholine-activated K(+) channels in mouse atrial myocytes. J Biol Chem 276(1):159–164. https://doi.org/10.1074/jbc.M004826200

Cho H, Lee D, Lee SH, Ho WK (2005) Receptor-induced depletion of phosphatidylinositol 4,5-bisphosphate inhibits inwardly rectifying K+ channels in a receptor-specific manner. Proc Natl Acad Sci USA 102(12):4643–4648. https://doi.org/10.1073/pnas.0408844102

Cho H, Kim YA, Ho WK (2006) Phosphate number and acyl chain length determine the subcellular location and lateral mobility of phosphoinositides. Mol Cells 22(1):97–103

Choveau FS, De la Rosa V, Bierbower SM, Hernandez CC, Shapiro MS (2018) Phosphatidylinositol 4,5-bisphosphate (PIP2) regulates KCNQ3 K(+) channels by interacting with four cytoplasmic channel domains. J Biol Chem 293(50):19411–19428. https://doi.org/10.1074/jbc.RA118.005401

Chung HJ, Qian X, Ehlers M, Jan YN, Jan LY (2009) Neuronal activity regulates phosphorylation-dependent surface delivery of G protein-activated inwardly rectifying potassium channels. Proc Natl Acad Sci USA 106(2):629–634. https://doi.org/10.1073/pnas.0811615106

Constanti A, Brown DA (1981) M-Currents in voltage-clamped mammalian sympathetic neurones. Neurosci Lett 24(3):289–294. https://doi.org/10.1016/0304-3940(81)90173-7

Cooper EC, Jan LY (2003) M-channels: neurological diseases, neuromodulation, and drug development. Arch Neurol 60(4):496–500. https://doi.org/10.1001/archneur.60.4.496

Cruzblanca H, Koh DS, Hille B (1998) Bradykinin inhibits M current via phospholipase C and Ca2+ release from IP3-sensitive Ca2+ stores in rat sympathetic neurons. Proc Natl Acad Sci USA 95(12):7151–7156. https://doi.org/10.1073/pnas.95.12.7151

Cui S, Ho WK, Kim ST, Cho H (2010) Agonist-induced localization of Gq-coupled receptors and G protein-gated inwardly rectifying K+ (GIRK) channels to caveolae determines receptor specificity of phosphatidylinositol 4,5-bisphosphate signaling. J Biol Chem 285(53):41732–41739. https://doi.org/10.1074/jbc.M110.153312

del Rio E, Bevilacqua JA, Marsh SJ, Halley P, Caulfield MP (1999) Muscarinic M1 receptors activate phosphoinositide turnover and Ca2+ mobilisation in rat sympathetic neurones, but this signalling pathway does not mediate M-current inhibition. J Physiol 520(Pt 1):101–111. https://doi.org/10.1111/j.1469-7793.1999.00101.x

Delmas P, Brown DA (2002) Junctional signaling microdomains: bridging the gap between the neuronal cell surface and Ca2+ stores. Neuron 36(5):787–790. https://doi.org/10.1016/s0896-6273(02)01097-8

Delmas P, Brown DA (2005) Pathways modulating neural KCNQ/M (Kv7) potassium channels. Nat Rev Neurosci 6(11):850–862. https://doi.org/10.1038/nrn1785

Delmas P, Wanaverbecq N, Abogadie FC, Mistry M, Brown DA (2002) Signaling microdomains define the specificity of receptor-mediated InsP(3) pathways in neurons. Neuron 34(2):209–220. https://doi.org/10.1016/s0896-6273(02)00641-4

Di Paolo G, De Camilli P (2006) Phosphoinositides in cell regulation and membrane dynamics. Nature 443(7112):651–657. https://doi.org/10.1038/nature05185

Dickson EJ, Falkenburger BH, Hille B (2013) Quantitative properties and receptor reserve of the IP(3) and calcium branch of G(q)-coupled receptor signaling. J Gen Physiol 141(5):521–535. https://doi.org/10.1085/jgp.201210886

Etxeberria A, Aivar P, Rodriguez-Alfaro JA, Alaimo A, Villace P, Gomez-Posada JC, Areso P, Villarroel A (2008) Calmodulin regulates the trafficking of KCNQ2 potassium channels. FASEB J 22(4):1135–1143. https://doi.org/10.1096/fj.07-9712com

Falkenburger BH, Dickson EJ, Hille B (2013) Quantitative properties and receptor reserve of the DAG and PKC branch of G(q)-coupled receptor signaling. J Gen Physiol 141(5):537–555. https://doi.org/10.1085/jgp.201210887

Ford CP, Stemkowski PL, Light PE, Smith PA (2003) Experiments to test the role of phosphatidylinositol 4,5-bisphosphate in neurotransmitter-induced M-channel closure in bullfrog sympathetic neurons. J Neurosci 23(12):4931–4941

Foucart S, Gibbons SJ, Brorson JR, Miller RJ (1995) Increase in [Ca2+]i by CCh in adult rat sympathetic neurons are not dependent on intracellular Ca2+ pools. Am J Physiol 268(4 Pt 1):C829-837. https://doi.org/10.1152/ajpcell.1995.268.4.C829

Gamper N, Shapiro MS (2003) Calmodulin mediates Ca2+-dependent modulation of M-type K+ channels. J Gen Physiol 122(1):17–31. https://doi.org/10.1085/jgp.200208783

Gamper N, Reznikov V, Yamada Y, Yang J, Shapiro MS (2004) Phosphatidylinositol [correction] 4,5-bisphosphate signals underlie receptor-specific Gq/11-mediated modulation of N-type Ca2+ channels. J Neurosci 24(48):10980–10992. https://doi.org/10.1523/JNEUROSCI.3869-04.2004

Gamper N, Li Y, Shapiro MS (2005) Structural requirements for differential sensitivity of KCNQ K+ channels to modulation by Ca2+/calmodulin. Mol Biol Cell 16(8):3538–3551. https://doi.org/10.1091/mbc.e04-09-0849

Geiser JR, van Tuinen D, Brockerhoff SE, Neff MM, Davis TN (1991) Can calmodulin function without binding calcium? Cell 65(6):949–959. https://doi.org/10.1016/0092-8674(91)90547-c

Grundy D (2015) Principles and standards for reporting animal experiments in the journal of physiology and experimental physiology. J Physiol 593(12):2547–2549. https://doi.org/10.1113/JP270818

Haley JE, Delmas P, Offermanns S, Abogadie FC, Simon MI, Buckley NJ, Brown DA (2000) Muscarinic inhibition of calcium

current and M current in Galpha q-deficient mice. J Neurosci 20(11):3973–3979

Herlitze S, Garcia DE, Mackie K, Hille B, Scheuer T, Catterall WA (1996) Modulation of Ca2+ channels by G-protein beta gamma subunits. Nature 380(6571):258–262. https://doi.org/10.1038/380258a0

Hernandez CC, Zaika O, Shapiro MS (2008a) A carboxy-terminal inter-helix linker as the site of phosphatidylinositol 4,5-bisphosphate action on Kv7 (M-type) K+ channels. J Gen Physiol 132(3):361–381. https://doi.org/10.1085/jgp.200810007

Hernandez CC, Zaika O, Tolstykh GP, Shapiro MS (2008b) Regulation of neural KCNQ channels: signalling pathways, structural motifs and functional implications. J Physiol 586(7):1811–1821. https://doi.org/10.1113/jphysiol.2007.148304

Horowitz LF, Hirdes W, Suh BC, Hilgemann DW, Mackie K, Hille B (2005) Phospholipase C in living cells: activation, inhibition, Ca2+ requirement, and regulation of M current. J Gen Physiol 126(3):243–262. https://doi.org/10.1085/jgp.200509309

Hoshi N, Zhang JS, Omaki M, Takeuchi T, Yokoyama S, Wanaverbecq N, Langeberg LK, Yoneda Y, Scott JD, Brown DA, Higashida H (2003) AKAP150 signaling complex promotes suppression of the M-current by muscarinic agonists. Nat Neurosci 6(6):564–571. https://doi.org/10.1038/nn1062

Ikeda SR (1996) Voltage-dependent modulation of N-type calcium channels by G-protein beta gamma subunits. Nature 380(6571):255–258. https://doi.org/10.1038/380255a0

Irving AJ, Collingridge GL (1998) A characterization of muscarinic receptor-mediated intracellular Ca2+ mobilization in cultured rat hippocampal neurones. J Physiol 511(Pt 3):747–759. https://doi.org/10.1111/j.1469-7793.1998.747bg.x

Jones S, Brown DA, Milligan G, Willer E, Buckley NJ, Caulfield MP (1995) Bradykinin excites rat sympathetic neurons by inhibition of M current through a mechanism involving B2 receptors and G alpha q/11. Neuron 14(2):399–405. https://doi.org/10.1016/0896-6273(95)90295-3

Kammermeier PJ, Ikeda SR (1999) Expression of RGS2 alters the coupling of metabotropic glutamate receptor 1a to M-type K+ and N-type Ca2+ channels. Neuron 22(4):819–829. https://doi.org/10.1016/s0896-6273(00)80740-0

Kim HJ, Jeong MH, Kim KR, Jung CY, Lee SY, Kim H, Koh J, Vuong TA, Jung S, Yang H, Park SK, Choi D, Kim SH, Kang K, Sohn JW, Park JM, Jeon D, Koo SH, Ho WK, Kang JS, Kim ST, Cho H (2016) Protein arginine methylation facilitates KCNQ channel-PIP2 interaction leading to seizure suppression. Elife. https://doi.org/10.7554/eLife.17159

Kirkwood A, Simmons MA, Mather RJ, Lisman J (1991) Muscarinic suppression of the M-current is mediated by a rise in internal Ca2+ concentration. Neuron 6(6):1009–1014. https://doi.org/10.1016/0896-6273(91)90240-z

Koizumi S, Rosa P, Willars GB, Challiss RA, Taverna E, Francolini M, Bootman MD, Lipp P, Inoue K, Roder J, Jeromin A (2002) Mechanisms underlying the neuronal calcium sensor-1-evoked enhancement of exocytosis in PC12 cells. J Biol Chem 277(33):30315–30324. https://doi.org/10.1074/jbc.M201132200

Kosenko A, Hoshi N (2013) A change in configuration of the calmodulin-KCNQ channel complex underlies Ca2+-dependent modulation of KCNQ channel activity. PLoS ONE 8(12):e82290. https://doi.org/10.1371/journal.pone.0082290

Kosenko A, Kang S, Smith IM, Greene DL, Langeberg LK, Scott JD, Hoshi N (2012) Coordinated signal integration at the M-type potassium channel upon muscarinic stimulation. EMBO J 31(14):3147–3156. https://doi.org/10.1038/emboj.2012.156

Kruse M, Whitten RJ (2021) Control of neuronal excitability by cell surface receptor density and phosphoinositide metabolism. Front Pharmacol 12:663840. https://doi.org/10.3389/fphar.2021.663840

Lee SY, Choi HK, Kim ST, Chung S, Park MK, Cho JH, Ho WK, Cho H (2010) Cholesterol inhibits M-type K+ channels via protein kinase C-dependent phosphorylation in sympathetic neurons. J Biol Chem 285(14):10939–10950. https://doi.org/10.1074/jbc.M109.048868

Li Y, Gamper N, Hilgemann DW, Shapiro MS (2005) Regulation of Kv7 (KCNQ) K+ channel open probability by phosphatidylinositol 4,5-bisphosphate. J Neurosci 25(43):9825–9835. https://doi.org/10.1523/JNEUROSCI.2597-05.2005

Meijer M, Hamers T, Westerink RHS (2014) Acute disturbance of calcium homeostasis in PC12 cells as a novel mechanism of action for (sub)micromolar concentrations of organophosphate insecticides. Neurotoxicology 43:110–116. https://doi.org/10.1016/j.neuro.2014.01.008

Meyer T, Wellner-Kienitz MC, Biewald A, Bender K, Eickel A, Pott L (2001) Depletion of phosphatidylinositol 4,5-bisphosphate by activation of phospholipase C-coupled receptors causes slow inhibition but not desensitization of G protein-gated inward rectifier K+ current in atrial myocytes. J Biol Chem 276(8):5650–5658. https://doi.org/10.1074/jbc.M009179200

Naraghi M (1997) T-jump study of calcium binding kinetics of calcium chelators. Cell Calcium 22(4):255–268. https://doi.org/10.1016/s0143-4160(97)90064-6

Neher E (1998) Usefulness and limitations of linear approximations to the understanding of Ca++ signals. Cell Calcium 24(5–6):345–357. https://doi.org/10.1016/s0143-4160(98)90058-6

Qi Y, Wang J, Bomben VC, Li DP, Chen SR, Sun H, Xi Y, Reed JG, Cheng J, Pan HL, Noebels JL, Yeh ET (2014) Hyper-SUMOylation of the Kv7 potassium channel diminishes the M-current leading to seizures and sudden death. Neuron 83(5):1159–1171. https://doi.org/10.1016/j.neuron.2014.07.042

Rajebhosale M, Greenwood S, Vidugiriene J, Jeromin A, Hilfiker S (2003) Phosphatidylinositol 4-OH kinase is a downstream target of neuronal calcium sensor-1 in enhancing exocytosis in neuroendocrine cells. J Biol Chem 278(8):6075–6084. https://doi.org/10.1074/jbc.M204702200

Robbins J, Marsh SJ, Brown DA (2006) Probing the regulation of M (Kv7) potassium channels in intact neurons with membrane-targeted peptides. J Neurosci 26(30):7950–7961. https://doi.org/10.1523/JNEUROSCI.2138-06.2006

Schroeder BC, Kubisch C, Stein V, Jentsch TJ (1998) Moderate loss of function of cyclic-AMP-modulated KCNQ2/KCNQ3 K+ channels causes epilepsy. Nature 396(6712):687–690. https://doi.org/10.1038/25367

Schuetz F, Kumar S, Poronnik P, Adams DJ (2008) Regulation of the voltage-gated K(+) channels KCNQ2/3 and KCNQ3/5 by serum- and glucocorticoid-regulated kinase-1. Am J Physiol Cell Physiol 295(1):C73-80. https://doi.org/10.1152/ajpcell.00146.2008

Seymour-Laurent KJ, Barish ME (1995) Inositol 1,4,5-trisphosphate and ryanodine receptor distributions and patterns of acetylcholine- and caffeine-induced calcium release in cultured mouse hippocampal neurons. J Neurosci 15(4):2592–2608

Shapiro MS, Roche JP, Kaftan EJ, Cruzblanca H, Mackie K, Hille B (2000) Reconstitution of muscarinic modulation of the KCNQ2/KCNQ3 K(+) channels that underlie the neuronal M current. J Neurosci 20(5):1710–1721

Sohn JW, Lim A, Lee SH, Ho WK (2007) Decrease in PIP(2) channel interactions is the final common mechanism involved in PKC- and arachidonic acid-mediated inhibitions of GABA(B)-activated K+ current. J Physiol 582(Pt 3):1037–1046. https://doi.org/10.1113/jphysiol.2007.137265

Suh BC, Hille B (2002) Recovery from muscarinic modulation of M current channels requires phosphatidylinositol 4,5-bisphosphate synthesis. Neuron 35(3):507–520. https://doi.org/10.1016/s0896-6273(02)00790-0

Suh BC, Inoue T, Meyer T, Hille B (2006) Rapid chemically induced changes of PtdIns(4,5)P2 gate KCNQ ion channels. Science 314(5804):1454–1457. https://doi.org/10.1126/science.1131163

Taverna E, Francolini M, Jeromin A, Hilfiker S, Roder J, Rosa P (2002) Neuronal calcium sensor 1 and phosphatidylinositol 4-OH kinase beta interact in neuronal cells and are translocated to membranes during nucleotide-evoked exocytosis. J Cell Sci 115(Pt 20):3909–3922. https://doi.org/10.1242/jcs.00072

Tsien RW, Lipscombe D, Madison DV, Bley KR, Fox AP (1988) Multiple types of neuronal calcium channels and their selective modulation. Trends Neurosci 11(10):431–438. https://doi.org/10.1016/0166-2236(88)90194-4

van Rheenen J, Jalink K (2002) Agonist-induced PIP(2) hydrolysis inhibits cortical actin dynamics: regulation at a global but not at a micrometer scale. Mol Biol Cell 13(9):3257–3267. https://doi.org/10.1091/mbc.e02-04-0231

Wang HS, Pan Z, Shi W, Brown BS, Wymore RS, Cohen IS, Dixon JE, McKinnon D (1998) KCNQ2 and KCNQ3 potassium channel subunits: molecular correlates of the M-channel. Science 282(5395):1890–1893. https://doi.org/10.1126/science.282.5395.1890

Winks JS, Hughes S, Filippov AK, Tatulian L, Abogadie FC, Brown DA, Marsh SJ (2005) Relationship between membrane phosphatidylinositol-4,5-bisphosphate and receptor-mediated inhibition of native neuronal M channels. J Neurosci 25(13):3400–3413. https://doi.org/10.1523/JNEUROSCI.3231-04.2005

Yoon J-Y (2010) Signaling mechanism of M current inhibition by M1 muscrinic receptor in rat sympathetic neurons. Seoul National University, Seoul, Korea

Zaika O, Tolstykh GP, Jaffe DB, Shapiro MS (2007) Inositol triphosphate-mediated Ca2+ signals direct purinergic P2Y receptor regulation of neuronal ion channels. J Neurosci 27(33):8914–8926. https://doi.org/10.1523/JNEUROSCI.1739-07.2007

Zaika O, Zhang J, Shapiro MS (2011) Combined phosphoinositide and Ca2+ signals mediating receptor specificity toward neuronal Ca2+ channels. J Biol Chem 286(1):830–841. https://doi.org/10.1074/jbc.M110.166033

Zhang H, Craciun LC, Mirshahi T, Rohacs T, Lopes CM, Jin T, Logothetis DE (2003) PIP(2) activates KCNQ channels, and its hydrolysis underlies receptor-mediated inhibition of M currents. Neuron 37(6):963–975. https://doi.org/10.1016/s0896-6273(03)00125-9

Zhao X, Varnai P, Tuymetova G, Balla A, Toth ZE, Oker-Blom C, Roder J, Jeromin A, Balla T (2001) Interaction of neuronal calcium sensor-1 (NCS-1) with phosphatidylinositol 4-kinase beta stimulates lipid kinase activity and affects membrane trafficking in COS-7 cells. J Biol Chem 276(43):40183–40189. https://doi.org/10.1074/jbc.M104048200